Phase behaviour and structural characterization of poly(1,3-propylene adipate)s with cyanoazobenzene side groups

E. L. Tassi; M. Paci; P. L. Magagnini; B. Yang; O. Francescangeli; F. Rustichelli

PLEASE SCROLL DOWN FOR ARTICLE

Phase behaviour and structural characterization of poly(1,3-propylene adipate)s with cyanoazobenzene side groups

by E. L. TASSI†, M. PACI†, P. L. MAGAGNINI*†, B. YANG‡, O. FRANCESCANGELI§ and F. RUSTICHELLI‡

†Dipartimento di Ingegneria Chimica, Chimica Industriale e Scienza dei Materiali, Università degli Studi di Pisa, via Diotisalvi 2, I-56126 Pisa, Italy
‡Istituto di Scienze Fisiche, and Istituto Nazionale per la Fisica della Materia, Università degli Studi di Ancona, via Ranieri 65, I-60131 Ancona, Italy
§Dipartimento di Scienze dei Materiali e della Terra, and Istituto Nazionale per la Fisica della Materia, Università degli Studi di Ancona, via Brecce Bianche, I-60131 Ancona, Italy

The phase behaviour and the structure of three poly(1,3-propylene adipate)s containing cyanoazobenzene side groups bonded to the backbone unit through flexible spacers with 6, 8 and 10 methylene groups have been studied by differential scanning calorimetry (DSC), polarized optical microscopy (POM) and X-ray diffraction (XRD) analysis. The polyadipates behave as enantiotropic side group liquid crystalline polymers. XRD analysis has shown that the organized phase of these polyadipates possesses a crystalline or a tilted structure of the SmF or SmG type. The temperature of fusion of this phase ($T_m \approx 45$–$48°C$) is almost independent of the length of the side group spacers. The crystalline phase can be obtained only by prolonged annealing at room temperature because crystallization from the melt is kinetically hindered. The range of thermodynamic stability ($T_i - T_m$) of the mesophase formed on melting increases with the length of the side group flexible spacers. The structure of the mesophase, determined by XRD, is of the smectic A type, and is characterized by a relatively large longitudinal displacement of the side groups, which is responsible for the unusually weak low angle Bragg reflections.

1. Introduction

The cyanoazobenzene group, which is known to be particularly useful for photo-induced orientation studies, has been employed by several workers as a mesogenic pendant for a number of side group liquid crystalline polymers (SGLCP) with polyacrylate/polymethacrylate [1–10], or polyester [11–13] main chains. A series of new liquid crystalline polyesters, based on aliphatic diacids and substituted propanediols carrying mesogenic cyanoazobenzene moieties, has been developed recently [14–16]. The structure of these polyesters (indicated herein as P*nam*, where P defines the 2-substituted 1,3-propanediol unit, *n* is the number of methylene groups in the side group spacer, **a** indicates that the azobenzene mesogen carries a cyano substituent in the *para*-position, and *m* is the number of methylene groups in the diacid unit) can be easily varied so as to change

the four parameters which were shown to influence the optical storage properties [17–19]. These are (1) the length of the methylene segment in the diacid moiety of the main chain; (2) the length of the side group spacer; (3) the substituent on the azobenzene mesogen; and (4) the molar mass. The phase behaviour of the P*nam* polyesters has been shown to be rather intricate, especially that of the homologues with *m* = 10–14. Thus, a DSC investigation of P8a12 showed that this polyester displays up to four partially overlapped endothermic effects on the heating scans, whose relative intensities change markedly with thermal history and measurement conditions [20]. These endotherms have been associated with the fusion of different organized phases which could not always be selectively developed by appropriate thermal treatments. For this reason, the structures of these phases could be investigated only preliminarily.

In this paper, the phase behaviour and the structures of three P*na*4 polyesters with *n* = 6, 8 and 10 are

*Author for correspondence.

described. The chemical structure of these polyadipates is shown below.
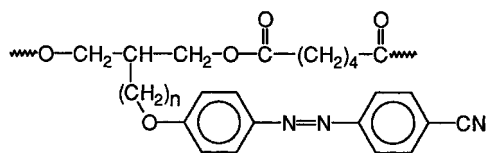
P*n*a4   (*n* = 6, 8, 10)

2. Experimental

The substituted poly(propylene adipate)s were synthesized according to a procedure described elsewhere [14–16], and were kindly provided by Dr F. Andruzzi. The intrinsic viscosities of the polyesters, measured in tetrahydrofuran at 30°C with an Ubbelohde viscometer, were 0·31, 0·33, and 0·30 dl g^{-1} for **P6a4**, **P8a4**, and **P10a4**, respectively. Thus, the molar masses of the investigated samples are very similar and allow their phase behaviour to be safely compared.

The thermal properties of **P*n*a4** have been studied by differential scanning calorimetry (DSC), using a DSC-4 Perkin Elmer apparatus. The DSC analysis of the **P*n*a4** polymers was carried out using one heating rate (3°C min^{-1}) and four different cooling rates (0·2, 3, 10 and 40°C min^{-1}). In some instances, additional traces were obtained on specimens having different thermal histories, e.g. specimens annealed for prolonged time intervals at appropriate temperatures.

The textures of thin polyester films were observed at room temperature using a Leitz Ortholux Pol-BK polarizing microscope. The films (0·5–5 μm thickness) were prepared on thoroughly cleaned microscope slides and were obtained by the following procedure. A few drops of a dilute (∼2 mg ml^{-1}) chloroform solution of the polyester were placed on the edge of a glass slide leaning on a second inclined slide. The upper glass slide was then dragged down slowly and the LCP solution was thus smeared on the inclined slide. Fairly uniform films were obtained after solvent evaporation under vacuum. The glass slides with the polyester films were placed in the hot stage (Mettler FP-52) of the polarizing microscope equipped with a Mettler FP-5 temperature controller, and the temperature was raised to 90–100°C to allow complete isotropization. The films were then cooled to room temperature using different rates, and the textures observed by switching on the polarized white light of reduced intensity for short time intervals.

Thermal optical analysis (TOA) was carried out by recording as a function of temperature the intensity of the light transmitted by the films, placed between crossed polarizers, by the use of a photocell placed on the

microscope eyepiece and connected to a recorder. For these measurements, the intensity of the light beam was set to a very low value (∼0·2 mW cm^{-2}), in order to minimize the textural changes induced by polarized light irradiation.

The structure of the liquid crystalline mesophase of **P*n*a4** was studied by X-ray diffraction (XRD). The measurements were performed using a Rigaku Denki RU300 rotating anode generator (40 kV, 200 mA) and Ni-filtered CuK$_\alpha$ radiation ($\lambda = 1\cdot54$ Å). The powder diffraction patterns were recorded at different temperatures between room temperature and the isotropization point by a conventional powder diffractometer in transmission geometry. The temperature of the sample was controlled within $\pm 0\cdot1$°C by a PDI temperature regulator. The fibre diffraction patterns were recorded at room temperature by using a pin-hole flat camera filled with helium gas to reduce air scattering.

3. Results and discussion
3.1. *DSC characterization*

The DSC traces of **P*n*a4** polyesters (scanning rate 3°C min^{-1}) are shown in figures 1 and 2. The specimens had been stored at room temperature for several weeks, after the precipitation and drying treatments, before these measurements. The first heating traces of these 'annealed' samples (figure 1) display two endothermic effects with maxima at T_m and T_i (for **P6a4** the latter endothermic peak is split). In contrast, on cooling and on reheating (figure 2), only the higher temperature transition is visible, in addition to the glass transition at $T_g \approx 10$°C. It is noteworthy that the glass transition is practically unidentifiable in the first run heating traces shown in figure 1. This demonstrates that the organization undergone by the polymer upon room temperature annealing leads, on the one hand, to the formation of a new phase melting at T_m, and, on the other, to the disappearance of the trace jump connected with the glass transition. It can be concluded, therefore, that the organized phase obtained by annealing probably leaves very little material in the fully amorphous state.

The calorimetric data for the three **P*n*a4** polyesters are collected in table 1. The glass transition temperature is observed for all three polyesters at ∼10°C, and appears to be almost independent of the length of the side group spacers. There seems to be good evidence in the literature that microphase separation can take place in comb-shaped polymers where the side groups and the main chains are intrinsically incompatible, provided the mass ratio of the two components is not far from 50/50 [21]. This event is reported to be most favourable for polymers containing widely spaced aromatic side groups bonded via flexible spacers to a predominantly aliphatic main chain: this is just the molecular model typical for
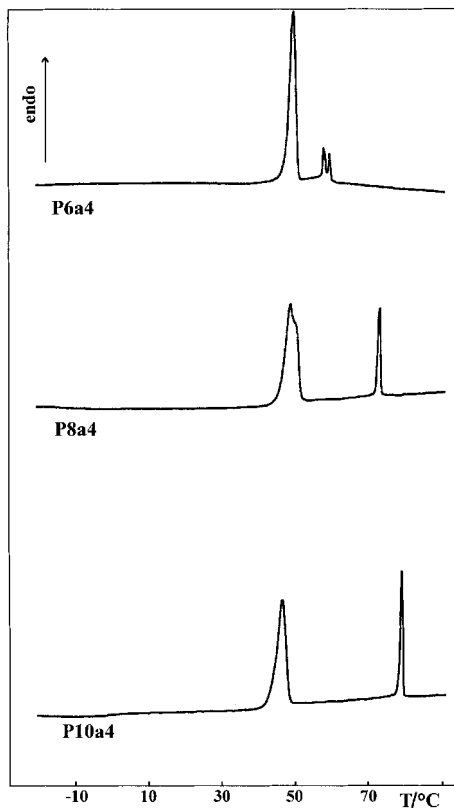
Figure 1.   First heating DSC traces of annealed **P***n***a4** polyesters.

Figure 2.   Rerun heating and cooling DSC traces of **P***n***a4** polyesters.

the presently investigated **P***n***a4** polyesters. A microphase segregation of this kind is expected to be revealed by the appearance of two glass transitions: that of the aromatic phase at a higher temperature, and that of the phase made up of aliphatic main chains and spacers at a lower temperature. Actually, for unsubstituted poly(1,3-propylene adipate) the glass transition temperature has been reported to be $-69°C$ [22]. Therefore, if a microphase segregation did actually take place for **P***n***a4**, a second glass transition should be discovered at lower temperatures, in addition to that clearly observed at *c.* 10°C. For this reason, accurate DSC measurements were repeated for **P8a4** over a temperature range from -100 to $+100°C$. However, only one baseline jump could be noticed at 10°C, as already discussed. It may be concluded, therefore, that **P***n***a4** polyesters do not give rise to any appreciable microphase segregation.

The first order transition taking place at T_m can be tentatively associated with the fusion of a crystalline (or ordered smectic) phase on the basis of the enthalpy change. The values of T_m and ΔH_m (45–48°C and 4–5 cal g^{-1}, respectively) appear almost independent of the chemical structure of the polyesters. However, as it is shown in table 1, only the DSC heating traces of annealed polymers display this transition. No evidence of the presence of a crystalline phase could be found in
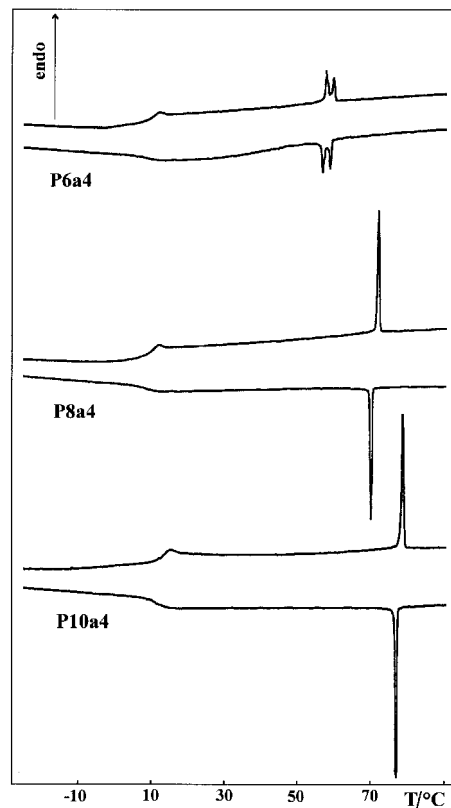
any of the rerun heating scans, whatever the rate of the previous cooling cycle. This demonstrates that the kinetics of crystallization of these polyesters is highly hindered. The crystalline structure could actually be developed to an appreciable extent only after prolonged storage of the specimens at nearly ambient temperature, and the process was shown to be much faster for **P8a4** than for the two other homologues. This is demonstrated in figure 3 where the enthalpies of fusion (ΔH_m) measured on polyester samples that were left at room temperature (25–35°C) after being cooled from 90°C are plotted against storage time. Whereas for **P8a4** appreciable crystallization takes place after ~ 10 h standing at *c.* 35°C, much longer storage times, ~ 300 and ~ 600 h, are needed for **P6a4** and **P10a4**, respectively, in order to get comparable crystallization. However, despite the quantitative differences in the crystallization kinetics, these data demonstrate that, for all three polyadipates, the organized structures whose range of thermodynamic stability is between T_m and T_i, may actually be stabilized for fairly long times at temperatures lower than T_m by simply cooling them at a normal rate from the molten state.

The first order transition taking place at T_i is affected by a fairly small degree of undercooling, as is expected

Table 1. Thermal characteristics of **P*n*a4** as measured by DSC.

Trace	Rate/°C min^{-1}	T_g/°C	T_m/°C	T_i/°C	ΔH_m/cal g^{-1}	ΔH_i/cal g^{-1}
P6a4						
1st heat	3	—	45·4	58·3, 60·2	4·73	0·39, 0·28
1st cool	−3	∼9	—	57·0, 58·1	—	0·40, 0·29
2nd heat	3	∼8	—	58·2, 60·2	—	0·42, 0·31
2nd cool	−10	∼10	—	56·3, 57·6	—	0·42, 0·35
3rd heat	3	∼8	—	58·2, 60·2	—	0·45, 0·32
3rd cool	−40	∼7	—	53·3[a]	—	0·78[a]
4th heat	3	∼9	—	58·2, 60·2	—	0·46, 0·32
P8a4						
1st heat	3	—	48·4	72·8	5·03	1·25
1st cool	−3	∼8	—	70·6	—	1·03
2nd heat	3	∼10	—	72·6	—	1·03
2nd cool	−10	∼9	—	69·7	—	1·07
3rd heat	3	∼9	—	72·6	—	1·07
3rd cool	−40	∼8	—	65·7	—	1·11
4th heat	3	∼10	—	72·7	—	1·10
P10a4						
1st heat	3	—	46·5	79·1	4·19	1·46
1st cool	−3	∼11	—	76·9	—	1·36
2nd heat	3	∼11	—	79·0	—	1·40
2nd cool	−10	∼10	—	76·1	—	1·52
3rd heat	3	∼12	—	79·1	—	1·32
3rd cool	−40	∼9	—	72·8	—	1·45
4th heat	3	∼13	—	79·0	—	1·37

[a] Single peak exotherm with shoulder on the high temperature side.
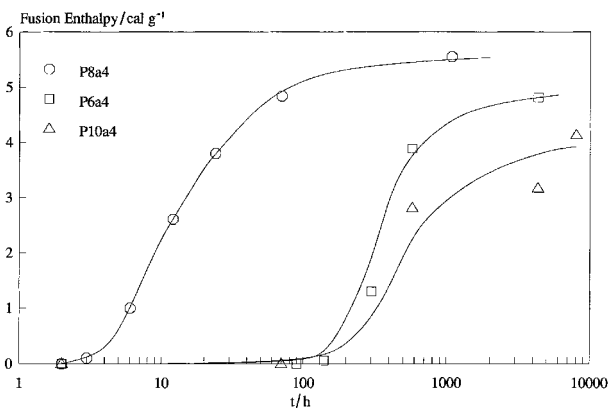
Figure 3. Fusion enthalpies of **P*n*a4** polyester samples vs time of annealing at 25–30°C.

for a mesophase↔isotropic transition. Both the temperature and the enthalpy change of this transition increase appreciably with the length of the side group spacers. In particular, for **P10a4** the transition enthalpy ($\Delta H_i \approx 1\cdot4$ cal g^{-1} or 765 cal mol^{-1}) is almost twice that measured for **P6a4** ($\Delta H_i \approx 0\cdot7$ cal g^{-1} or 345 cal mol^{-1}). This difference can be reasonably accounted for by assuming that the four added methylenes bring about a better organization of the whole mesophase of **P10a4**, as compared with that of **P6a4**, rather than merely contri-

buting their own enthalpy content. On the other hand, this conclusion is in agreement with the much higher isotropization entropy of **P10a4** ($\Delta S_i \approx 2\cdot17$ cal K^{-1} mol^{-1}, versus $\Delta S_i \approx 1\cdot04$ cal K^{-1} mol^{-1} for **P6a4**).

3.2. *POM characterization*

It is well known that irradiation of films of SGLCPs containing azobenzene side groups with polarized light of appropriate wavelength causes *trans↔cis* isomerization and, thereby, alignment of the azobenzenes in a direction perpendicular to the polarization direction of the impinging beam [23]. The side group orientation due to polarized light causes important textural changes. For this reason, the textures of the mesophases of **P*n*a4** could be observed reliably only at low temperatures, and with relatively low light intensities, in order to make the reorientation phenomena sufficiently slow.

The phase behaviour of the polyesters could not be safely assessed by direct observation of the textural changes undergone by thin films of these materials during cooling/heating runs carried out on the hot stage of a polarizing microscope because of the concurrent effects due to the azobenzene orientation induced by the light beam. For example, if an annealed film of **P8a4** was observed using crossed polarizers while heating it from room temperature under medium intensity illumination,

a complete destruction of the texture could be seen in the region of the melting point (T_m), and the field appeared uniformly dark above this temperature, as if premature isotropization had taken place. However, the use of very weak polarized white light beam ($\sim 0.2\ \mathrm{mW\ cm^{-2}}$) allowed the phase transitions of these polyesters to be monitored microscopically by the thermal optical analysis (TOA) technique, as described in the experimental section. In fact under these irradiation conditions, practically no reorientation of the azobenzene moieties takes place during measurement, except perhaps at temperatures very close to T_i, and the intensity transmitted by the polyester film through crossed polarizers could be recorded as a function of temperature with a photocell placed on the eyepiece of the polarizing microscope. The textural changes undergone by the polyesters, and corresponding to the phase transitions, can therefore be monitored as changes of the transmitted light intensity. The TOA curves measured for the three polyesters during a series of heating–cooling cycles run at $3°\mathrm{C\ min^{-1}}$ are shown in figures 4–6. Before measurement the films had been stored at room temperature for
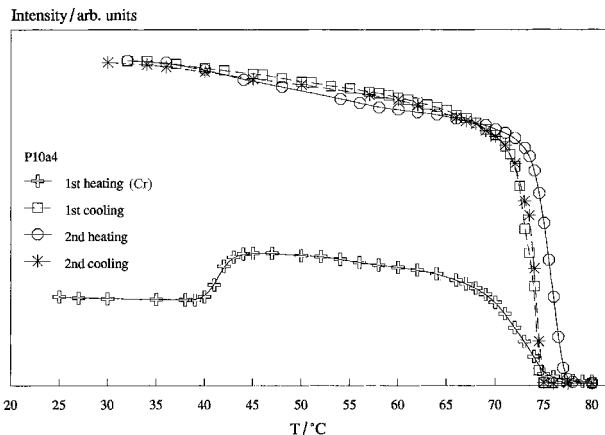

Figure 6.   TOA curves for a thin film of the **P10a4** polyester.

several months and, therefore, according to the results of the calorimetric analysis discussed before, the polyesters were in the crystalline state (Cr) at the moment of the first heating cycle. The first run TOA traces for all three polyesters show, corresponding to the fusion of the crystalline phase, an increase of transmitted intensity. A comparison of the temperature intervals of the DSC melting transitions, taken as the width of the endothermic peaks on the trace baseline, and those wherein the rise in the TOA curves is observed, shows that there is reasonable agreement between the data obtained using the two techniques (cf. table 2).

The dramatic drop in transmitted light intensity observed at higher temperatures (cf. figures 4–6) is clearly correlated with the isotropization transition of the polyesters. It is noteworthy that, once the crystalline phase was destroyed, practically identical TOA curves were obtained on rerunning, thus confirming that the m↔i transition is reproducible and characterized by a fairly small degree of undercooling. For the purpose of the present discussion, it may be interesting to compare the isotropization intervals found by DSC with the temperatures corresponding to complete extinction in the TOA curves. The relevant figures are also collected in table 2. The values found by TOA are *c.* 2, 4 and 6°C
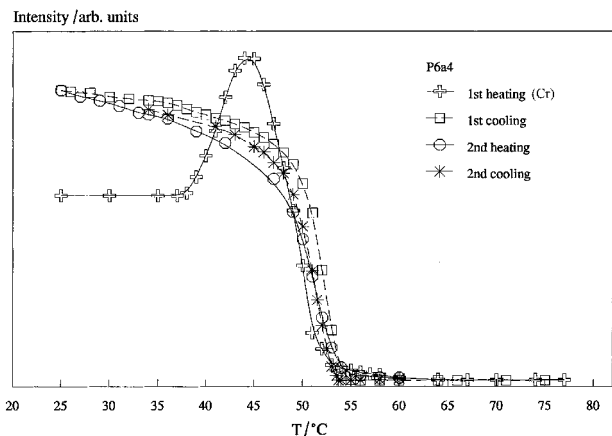
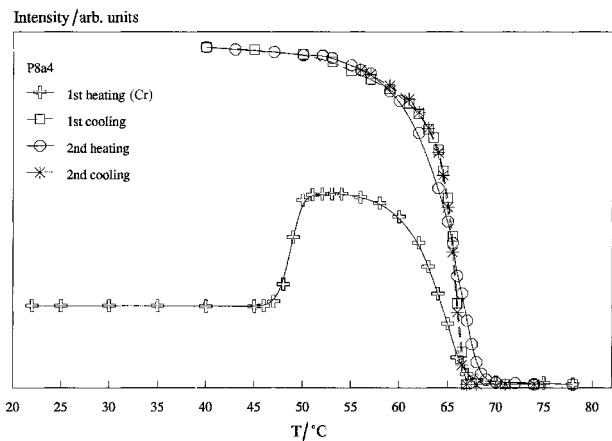

Figure 4.   TOA curves for a thin film of the **P6a4** polyester.

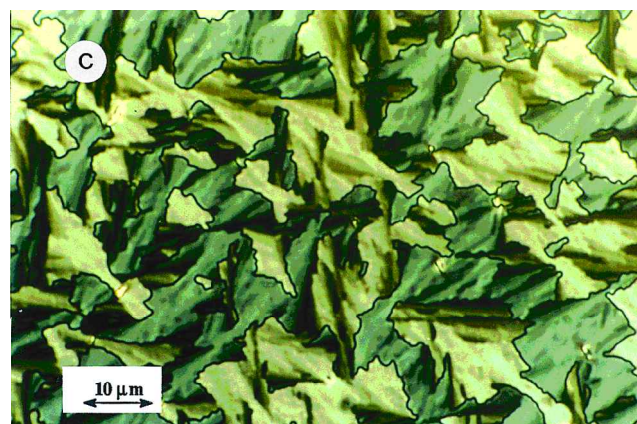Figure 5.   TOA curves for a thin film of the **P8a4** polyester.

Table 2.   Temperature intervals (°C) of fusion and isotropization, as measured by DSC and TOA.

Technique	**P6a4**	**P8a4**	**P10a4**
Fusion intervals			
DSC	41·5–47·5	44·5–51·5	42·5–49·0
TOA[a]	39·0–45·0	46·0–50·0	40·0–45·0
Isotropization intervals			
DSC	56·5–61·0	71·0–73·0	77·0–79·0
TOA[a]	53·0	68·0	76·0

[a] Polarized white light illumination with a beam intensity of $\sim 0.2\ \mathrm{mW\ cm^{-2}}$.

Figure 8. Textures ($\times 630$) of thin films of (*a*) **P8a4**, and (*b*) **P10a4**, as in figure 7, after several days annealing at $\sim 30°C$.
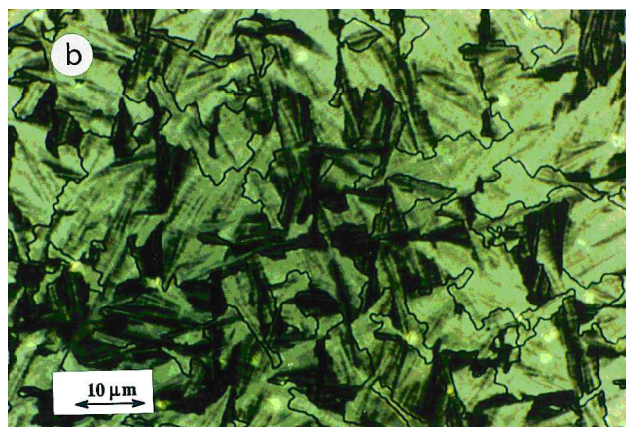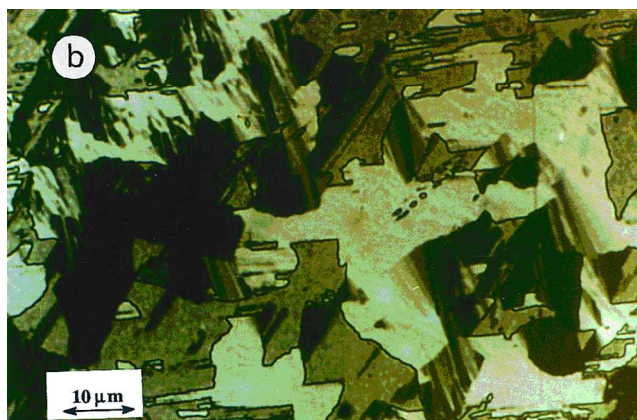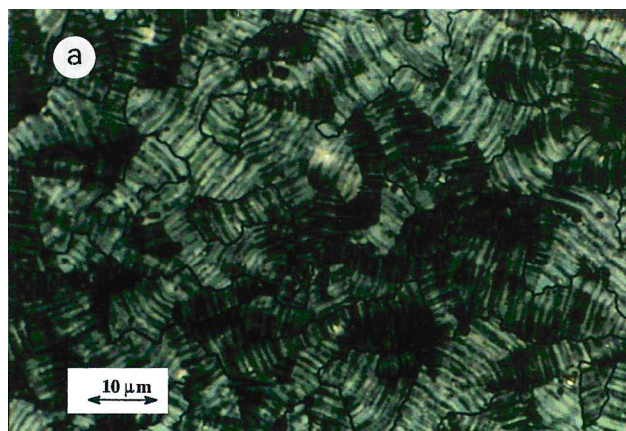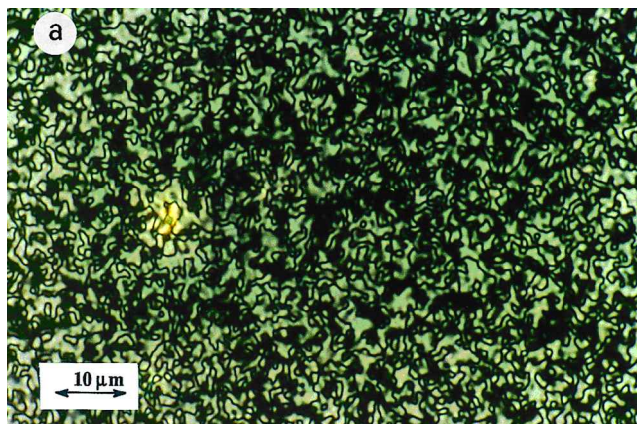
Figure 7. Textures ($\times 630$) of thin films of (*a*) **P6a4**, (*b*) **P8a4** and (*c*) **P10a4**, cooled in the dark from the isotropic state at a rate of $0·2°C\,min^{-1}$.

mobility is high. It may be interesting to note that this phenomenon of premature apparent isotropization is more evident the shorter the side group spacers of the polyesters.

The textures observed at room temperature for thick ($>c.$ 5 μm) polymer films were invariably of the 'fine grain' or 'tight' type, as were those of thinner films previously cooled at an appreciable rate from the isotropic state. The 'tight' texture is interpreted as the result of a relatively high nucleation density, which leads to ordered domains of very small dimensions. The morphology of films displaying this type of texture even at high magnification can hardly be resolved. However, after very slow ($0·2°C\,min^{-1}$) cooling from the isotropic state to room temperature, thin ($0·5–5$ μm) films of the polyesters displayed the textures shown in figure 7. **P6a4** always produced fairly 'tight' textures [cf. figure 7(*a*)] whereas for both **P8a4** and **P10a4** much larger domains were visible [cf. figures 7(*b*) and 7(*c*)]. The textures of the latter polymers may probably be attributed to smectic phases, although this assignment is not unambiguous.

lower than the average DSC values (T_i), for **P10a4**, **P8a4** and **P6a4**, respectively. This is thought to be due to the effect of the polarized light beam, which, despite the very low intensity, may orient the azobenzene group in a direction perpendicular to the polarization direction when the temperature is close to T_i and the molecular
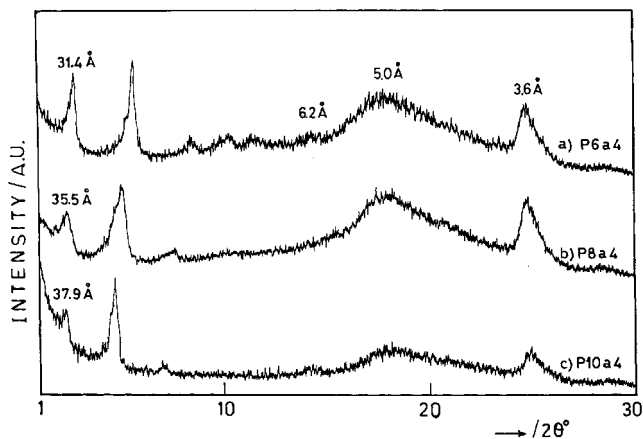
Figure 9. XRD spectra taken at room temperature on powder samples of **P*n*a4** polyesters in the crystalline state (annealed at nearly room temperature for several days).

Figure 11. XRD spectra taken at $T = 50°C$ on powder samples of **P*n*a4** polyesters.

The effect of thermal history (annealing treatments) on the textures displayed by thin films of the polyesters is illustrated in figures 8 (*a*) and 8 (*b*) for **P8a4** and **P10a4**, respectively. A prolonged annealing (one month at *c.* 25°C) of a **P8a4** film leads to a progressive appearance of a banded texture within the domains [figure 8 (*a*)]. This texture is attributed to the crystalline (or ordered smectic) phase of this polyadipate. The change undergone by the texture of a **P10a4** film as a result of room temperature annealing is comparatively smaller [compare figures 7 (*c*) and 8 (*b*)], and this is in agreement with the DSC data indicating that the crystallization of **P10a4** takes place at a considerably lower rate compared with **P8a4**. A prolonged annealing of the **P6a4** film failed

to cause appreciable changes of the texture shown in figure 7 (*a*).

3.3. *X-ray diffraction characterization*
3.3.1. *Crystalline phase*

Figure 9 shows the room temperature powder diffraction spectra of polyesters **P6a4**, **P8a4** and **P10a4**, in the crystalline (annealed) state. The spectra are very similar and feature three sharp diffraction peaks in the low angle region ($2\theta = 2·81°$, $5·62°$ and $8·43°$, for **P6a4**; $2·48°$, $4·97°$, and $7·46°$, for **P8a4**; $2·33°$, $4·68°$ and $7·00°$, for **P10a4**) whose spacings are in the ratio $1:2:3$. In addition, two diffraction peaks (one very weak, and the other strong, corresponding to spacings of $6·2$ and $3·6$ Å, respectively are observed in the high angle region, together with a wide diffuse halo centred at about $4·9$ Å.
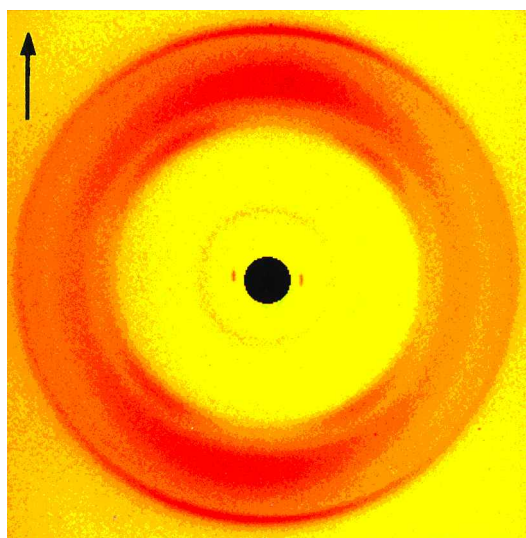

Figure 10. XRD pattern of a fibre sample of the **P10a4** polyester in the crystalline state (annealed at nearly room temperature for several days). The arrow indicates the fibre axis direction.
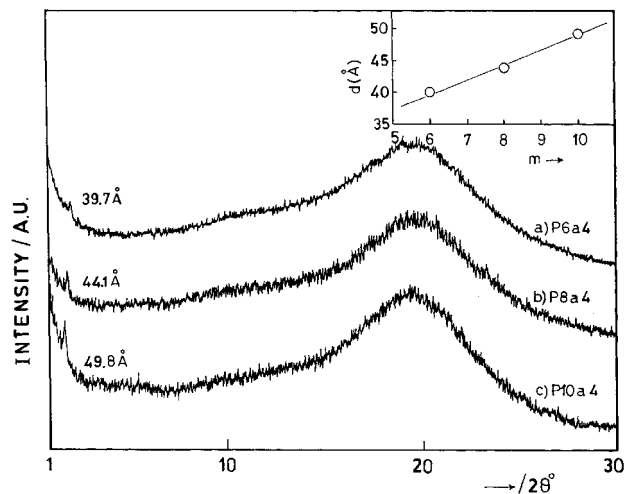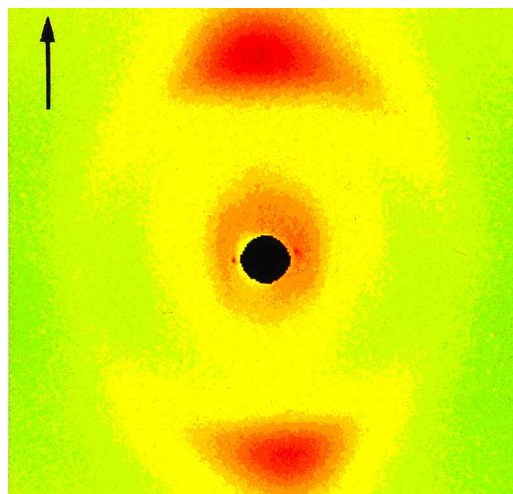

Figure 12. XRD pattern of a fibre sample of the **P10a4** polyester, in the mesophase. The arrow indicates the fibre axis direction.

The low angle reflections indicate that the crystalline phases of the polyesters exhibit a well ordered lamellar structure with layer spacings equal to 31·4, 35·5, and 37·9 Å, respectively, while the high angle reflections are associated with the molecular packing within the layers.

In order to obtain further information on the structure of these polyadipates, we recorded a diffraction pattern of an oriented sample of **P10a4** in the crystalline phase (cf. figure 10). The four wide-angle diffuse signals equidistant from the origin, and forming pairs on straight lines at an angle $\beta = 45°$ to the fibre axis, point to the occurrence of either a crystalline phase or a tilted phase of the smectic F or the G type.

3.3.2. *Mesophase*

The powder diffraction spectra of polyesters **P6a4**, **P8a4**, and **P10a4** taken at about 50°C, i.e. a temperature within the range of stability of the mesophases, are shown in figure 11. These spectra exhibit a sharp low angle peak and a wide angle diffuse halo, which are characteristic of a disordered smectic mesophase. The layer spacings d calculated from the positions of the low angle sharp peaks are 39·7, 44·1 and 49·8 Å, respectively. It should be noted that the thickness d of the smectic layers is approximately twice the length of the side group in the fully extended conformation. In addition, the slope of the straight line interpolating the experimental data on a d versus m plot (cf. the inset of figure 11) corresponds to 2·5 Å per methylene group. These results are consistent with a bilayer SmA mesophase.

In order to confirm the bilayer SmA structure of the mesophase of the polyesters, the diffraction pattern of an oriented specimen of **P10a4** in the mesomorphic state was recorded. The sample was prepared by stretching a fibre at about 60°C and rapidly cooling it in air. The measurement was performed at room temperature, just after quenching. In these conditions, the fibre is in the mesophase since, as discussed before, crystallization requires annealing times of several weeks. The diffraction pattern of the oriented mesophase of **P10a4** is shown in figure 12. It displays two sharp reflections, corresponding to a d spacing of ~ 50 Å, in the small angle region, located on the equatorial line (i.e. normal to the fibre axis) and symmetrically placed with respect to the origin, and a diffuse wide angle crescent, centred at about 4·6 Å on the meridional line. This pattern confirms that the polymer forms a SmA mesophase with a d spacing of 50 Å, corresponding to a bilayer arrangement of the side groups. The fibre diffraction pattern also demonstrates that the main chains and the smectic layer planes are aligned parallel to the fibre axis, whereas the side groups are aligned normal to it.

Rather surprisingly, the intensity of the low angle Bragg reflection is unusually low if compared with that of the high angle diffuse halo. However, the reflection is sharp, and this indicates the existence of long range positional order along the smectic layer normal direction. This experimental evidence can be explained in terms of a poor electron density contrast along the normal to the smectic layers. In fact, as the distance between two adjacent side groups linking points in the fully extended main chain is much larger than the diameter of the side group cross section, the main chains should be strongly folded in the smectic layers, thus allowing a relatively large longitudinal displacement of the side groups. Such displacements reduce the electron density contrast along the longitudinal direction and, consequently, the intensity of the Bragg peak associated with the reflection on the smectic planes.

A schematic representation of the macromolecular organization in the mesophase is shown in figure 13. This picture underlines the appreciably lower translational order exhibited by this mesophase, as compared with that usually encountered in SmA phases.

4. Conclusions

The phase behaviour of **P*n*a4** polyesters is typical for enantiotropic SGLCPs. When appropriately annealed at room temperature, they develop highly ordered smectic (probably SmF or SmG) or crystalline phases that give rise, upon heating, to endothermic peaks of fusion at T_m, in the 45–48°C range. Both the temperatures and the enthalpies of fusion of the crystalline phases are
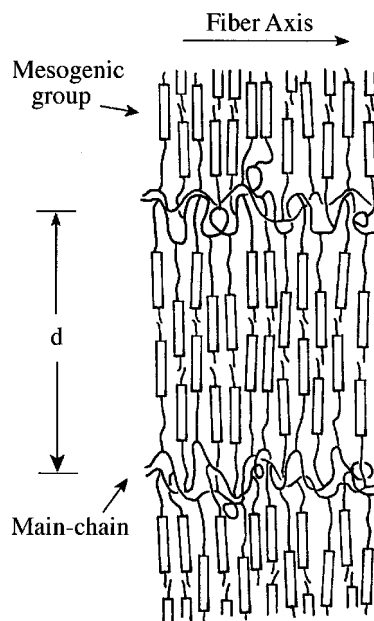

Figure 13. Schematic representation of the molecular organization of the **P*n*a4** polyesters in the bilayer SmA phase.

almost independent of the length of the side group spacers. Upon cooling from the isotropic state, a meso-phase is formed at $T_i > T_m$. The range of thermodynamic stability of the mesophase ($T_m < T < T_i$) is wider the longer the side group spacers. However, due to the hindered kinetics of crystallization, the mesophases of **P*n*a4** are stable for fairly long times even at room temperature. The XRD analysis of the mesophases of these polyesters has shown that their structure is typical for a bilayer SmA liquid crystal characterized by a relatively large longitudinal displacement of the side groups, which is responsible for the unusually low intensity of the low angle Bragg reflections.

References

[1] RINGSDORF, H., and SCHMIDT, H. W., 1984, *Makromol. Chem.*, **185,** 1327.

[2] EICH, M., and WENDORFF, J. H., 1987, *Makromol. Chem., rapid Commun.*, **8,** 467.

[3] ANDERLE, K., BIRENHEIDE, R., EICH, M., and WENDORFF, J., 1989, *Makromol. Chem., rapid Commun.*, **10,** 477.

[4] WIESNER, U., ANTONIETTI, M., BOEFFEL, C., and SPIESS, H. W., 1990, *Makromol. Chem.*, **191,** 2133.

[5] EICH, M., and WENDORFF, J. H., 1990, *J. opt. Soc. Am., B*, **7,** 1428.

[6] ANDERLE, K., BIRENHEIDE, R., and WENDORFF, J. H., 1991, *Makromol. Chem., macromol. Symp.*, **44,** 11.

[7] WIESNER, U., REYNOLDS, N., BOEFFEL, C., and SPIESS, H. W., 1991, *Makromol. Chem., rapid Commun.*, **12,** 457.

[8] IVANOV, S., YAKOVLEV, I., KOSTROMIN, S., SHIBAEV, V., LAESKER, L., STUMPE, J., and KREISIG, D., 1991, *Makromol. Chem., rapid Commun.*, **12,** 709.

[9] ANDERLE, K., BIRENHEIDE, R., WERNER, M. J. A., and WENDORFF, J. H., 1991, *Liq. Cryst.*, **9,** 691.

[10] WIESNER, U., REYNOLDS, N., BOEFFEL, C., and SPIESS, H. W., 1992, *Liq. Cryst.*, **11,** 251.

[11] RECK, B., and RINGSDORF, H., 1985, *Makromol. Chem., rapid Commun.*, **6,** 291.

[12] EICH, M., WENDORFF, J. H., RECK, B., and RINGSDORF, H., 1987, *Makromol. Chem., rapid Commun.*, **8,** 59.

[13] RECK, B., and RINGSDORF, H., 1990, *Liq. Cryst.*, **8,** 247.

[14] HVILSTED, S., ANDRUZZI, F., and RAMANUJAM, P. S., 1992, *Opt. Lett.*, **17,** 1234.

[15] RAMANUJAM, P. S., HVILSTED, S., and ANDRUZZI, F., 1993, *Appl. Phys. Lett.*, **62,** 1041.

[16] HVILSTED, S., ANDRUZZI, F., KULINNA, C., SIESLER, H. W., and RAMANUJAM, P. S., 1995, *Macromolecules*, **28,** 2172.

[17] RAMANUJAM, P. S., HVILSTED, S., and ANDRUZZI, F., 1994, *Opt. Rev.*, **1,** 30.

[18] ZEBGER, I., KULINNA, C., SIESLER, H. W., ANDRUZZI, F., PEDERSEN, M., RAMANUJAM, P. S., and HVILSTED, S., 1995, *Macromol. Symp.*, **94,** 159.

[19] RAMANUJAM, P. S., HVILSTED, S., ZEBGER, I., and SIESLER, H. W., 1995, *Macromol. rapid Commun.*, **16,** 455.

[20] TASSI, E. L., PACI, M., and MAGAGNINI, P. L., 1995, *Mol. Cryst. liq. Cryst.*, **266,** 135.

[21] PERCEC, V., 1988, *Mol. Cryst. liq. Cryst.*, **155,** 1, and references therein.

[22] WOO, E. M., BARLOW, J. W., and PAUL, D. R., 1985, *Polymer*, **26,** 763.

[23] NATANSOHN, A., ROCHON, P., GOSSELIN, J., and XIE, S., 1992, *Macromolecules*, **25,** 2268.